Supporting Information: Enhanced Photodiodes with Coupled Organic-Inorganic Nanostructures Utilizing double Heterostructure ligands versus Single Ligand

Shaimaa M. Abdalbaqi*

Institut für Physik, Universität Augsburg, 86135 Augsburg, Germany

E-mail: shaimaa.abdalbaqi76@gmail.com

1 Absorption

Figure S1 a and b show the absorption spectra of pentacene and the purchased NCs of size (6.1+/- 0.9nm). The onset value of (1.8e.V) in Figure S1a corresponds to the optical energy gap of pentacene. Two peaks appear between (900 and 1300nm) for PbS-NCs in Figure S1b. These peaks represent the absorption of the higher energy levels of NCs. The main absorption of PbS-NC in the infrared range is slightly above (1600nm).

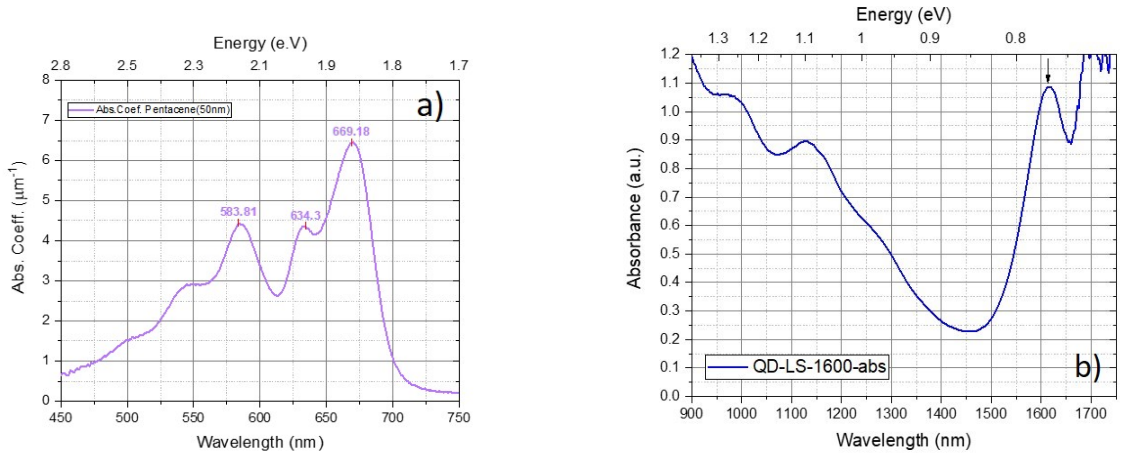

Figure S1: a) Measured absorption spectrum for pentacene b) Measured absorption spectrum for PbS-NCs.

2 Energy Levels, UPS and XPS

Figure S2 shows the ultraviolet photoelectron spectroscopy and X-ray photoelectron spectroscopy of the PbS-COINs with pentacene on PEDOT:PSS. The onset of secondary electron cut-off (SECO) at the low kinetic energy represents the work function after subtracting the sample bias during the measurement (-10 V). The valence region is shown for each sample on the linear and logarithmic scales. The onset of the semi-log plot represents the valence level ($1S_h$). The XPS spectra identify the elemental composition of the films qualitatively by matching the positions of the peaks to an element reference database.[?]

- pentacene/PEDOT:PSS

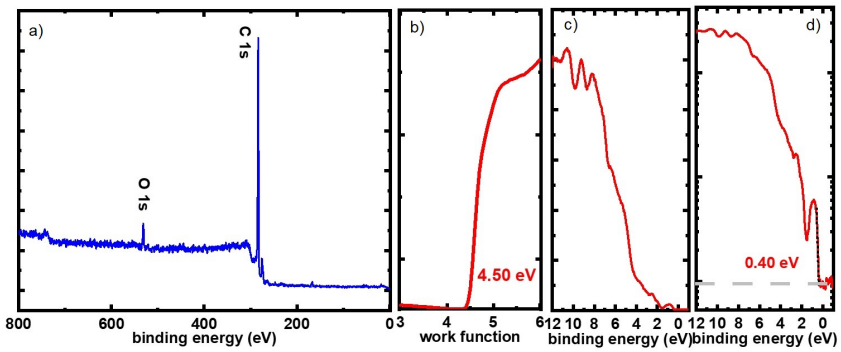

- PbS-EDT/pentacene/PEDOT:PSS

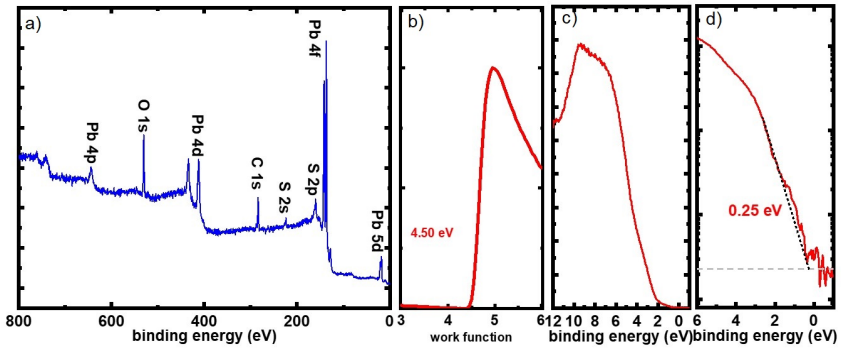

- PbS-TBAI/pentacene/PEDOT:PSS

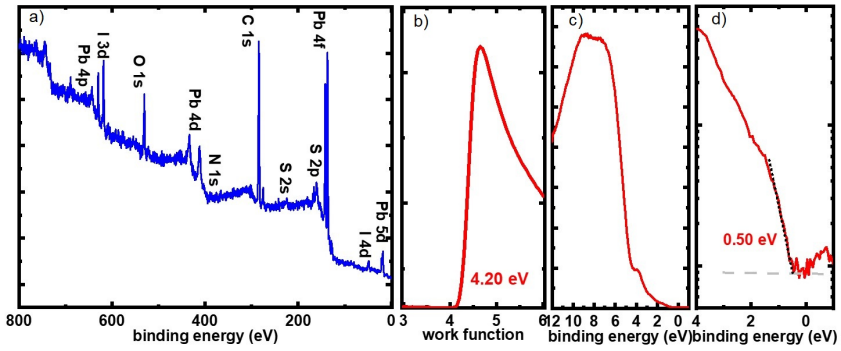

- PbS-TBAI/PbS-EDT/pentacene/PEDOT:PSS

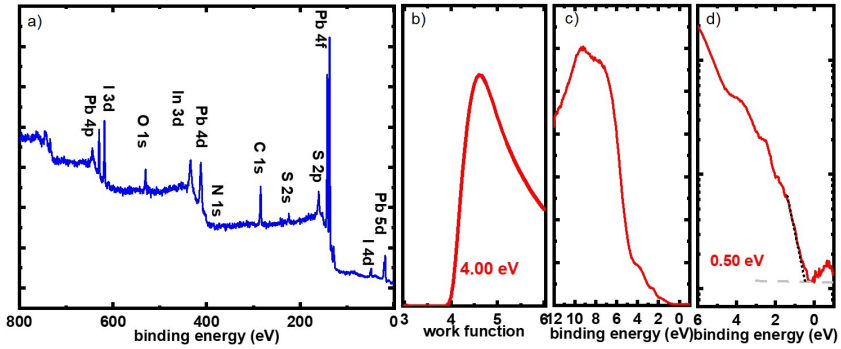

Figure S2: XPS and UPS spectra of PbS-EDT, PbS-TBAI and PbS-EDT/PbS-TBAI with pentacene. a) XPS spectrum, with assigned elemental orbitals for each peak b) SECO, c) and d) Linear and Semi-log of the valence onset.

3 Transmission Electron Microscope

In connection to the manuscript results, we measured the interparticle distances for different PbS-ligands from the real images of a scanning transmission electron microscope (STEM) and their fast Fourier transformation (FFT). Another option would be measuring these spaces using the same GATAN software and measuring the live profile by applying a straight line for several adjacent NCs. Figure S3 (a) exposes the PbS-OA image. It highlighted the first monolayer which has an ordered hexagonal lattice. The inter-particles' voids which are obtained from the real, FFT and live profile are given in Table S1. Inverted FFT could be used precisely to determine the distances of the live profile after applying a mask to selective bright diffraction spots. STEM images for PbS-EDT and PbS-TBAI are shown in Figure S5 and their interparticle distances are listed in Table S1. The interparticle distance (3.3nm) in Table S1 of OA appears to be the double size of the OA molecule (1.44 nm) which is measured according to Schrödinger software. However, the interparticle distances which are obtained from the FFT and the live profile apparently have different values.

In the case of PbS-EDT and TBAI, it is difficult to determine the interparticle distances.

However, the average interparticle distances in the case of EDT is almost equal to the EDT length because the PbS-NCs are attached directly to the ends of the ligands. In the case of TBAI, PbS-NCs are attached to the middle of the ligands. Therefore the average results of the interparticle distance is even more.

The STEM images of PbS-EDT and PbS-TBAI suggest a strong interaction between ligands and PbS-NCs. From the images, it is obvious that TBAI molecules attracted more NCs to substitute the sulfide ions in the PbS-NCs by the iodine ions of TBAI. This explains the large agglomerations which appear in their STEM images. Because the most reacted plane is (111) for PbS-NCs as mentioned in the manuscript, this observation is confirmed by the atomic resolution in the case of PbS-EDT and PbS-TBAI images. The atomic resolution of NCs in PbS-EDT and PbS-TBAI films are illustrated in Figures S6- S9. The FFT images of Figure S7 and S9 reveal more lattice planes which are listed in Table S2.

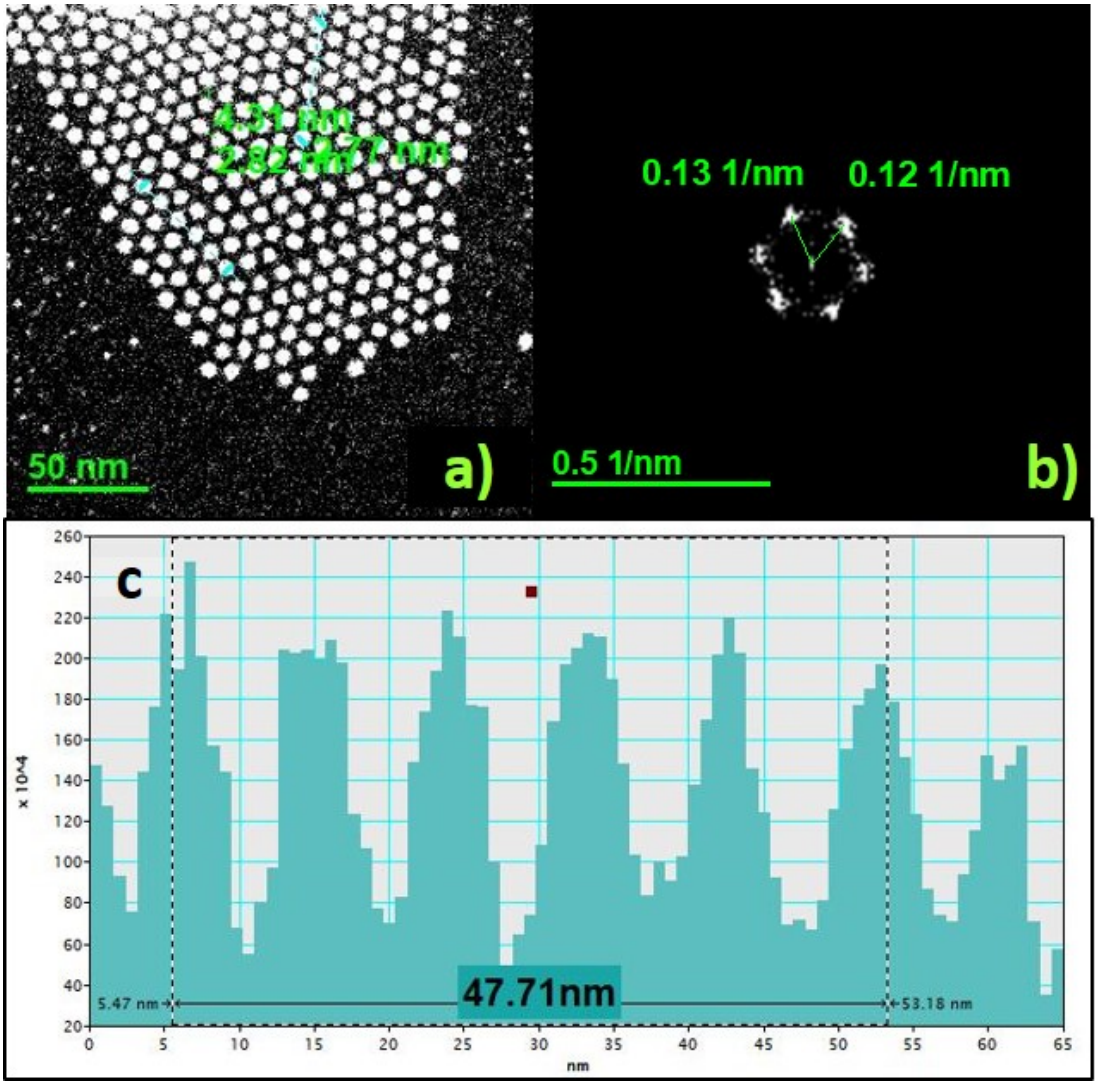

Figure S3: STEM images for PbS-NCs capped with a) oleic acid, b) FFT image c) live profile for the first monolayer.

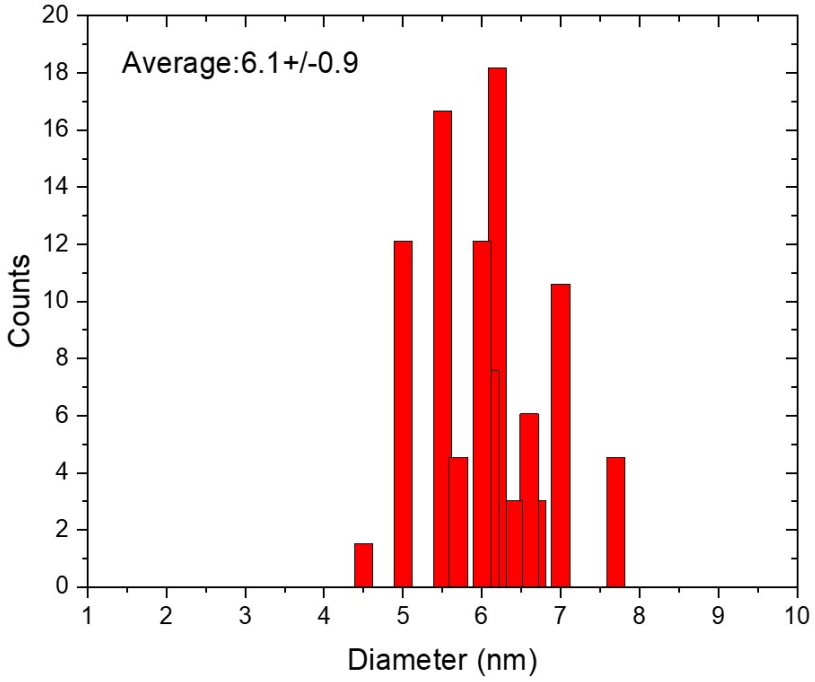

Figure S4: Corresponding normalized size distribution histogram of native OA-capped PbS-NCs

Table S1: List of interparticles' distances of different ligands.

$d_{\text{real image}}$ (nm)	FFT (1/nm)	$d_{1/\text{FFT}}$ (nm)	$d_{\text{live profile}}$ (nm)
PbS-OA			
3.3	0.12	8.3	1.342
	0.13	7.6	2.918
PbS-EDT			
0.53	0.16	6.3	0.85
0.7	0.26	3.8	3.85
	0.42	2.4	
PbS-TBAI			
1.37	0.15	6.6	1.78
1.48			
1.56			

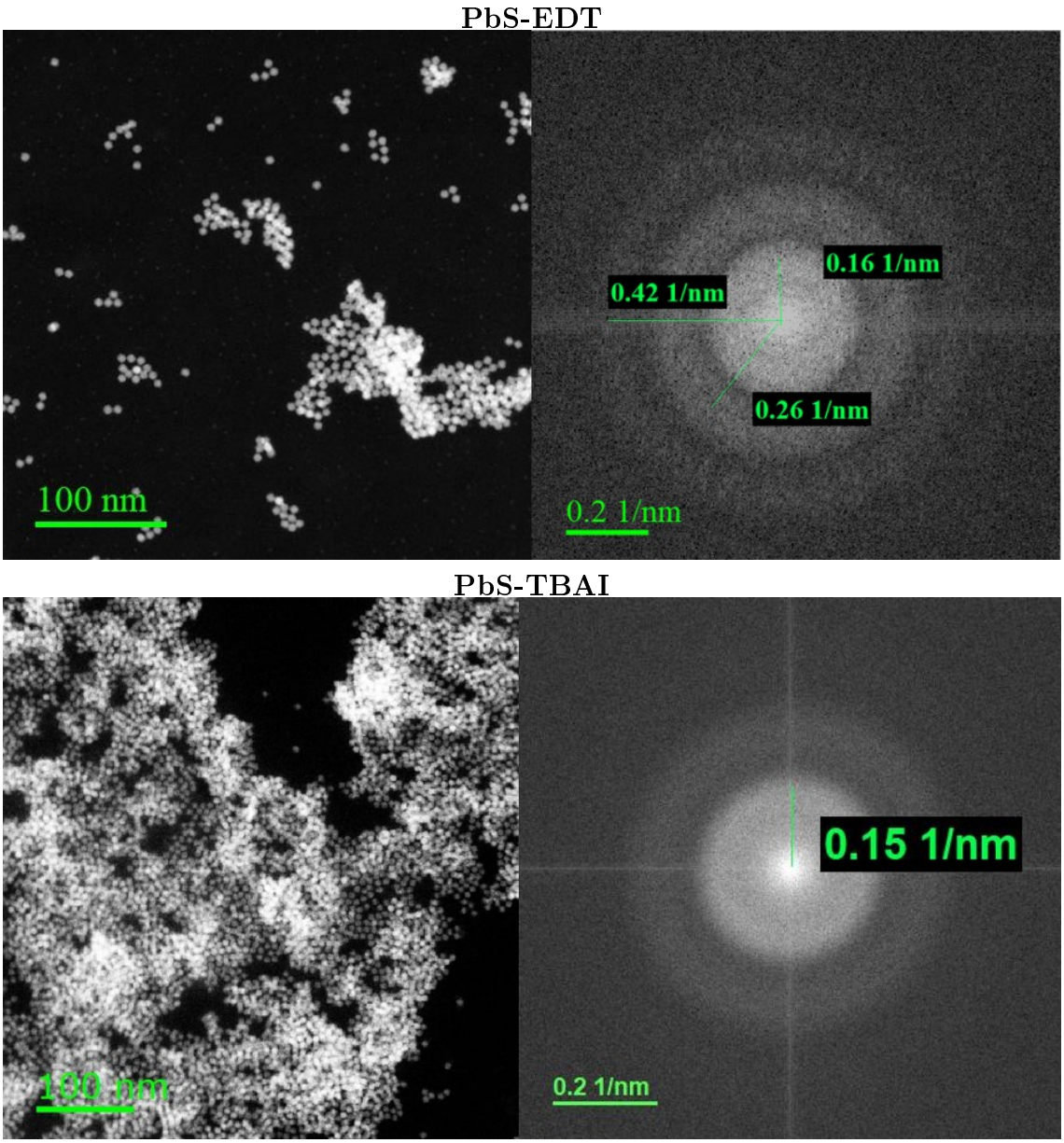

Figure S5: STEM and FFT images of PbS-EDT and PbS-TBAI.

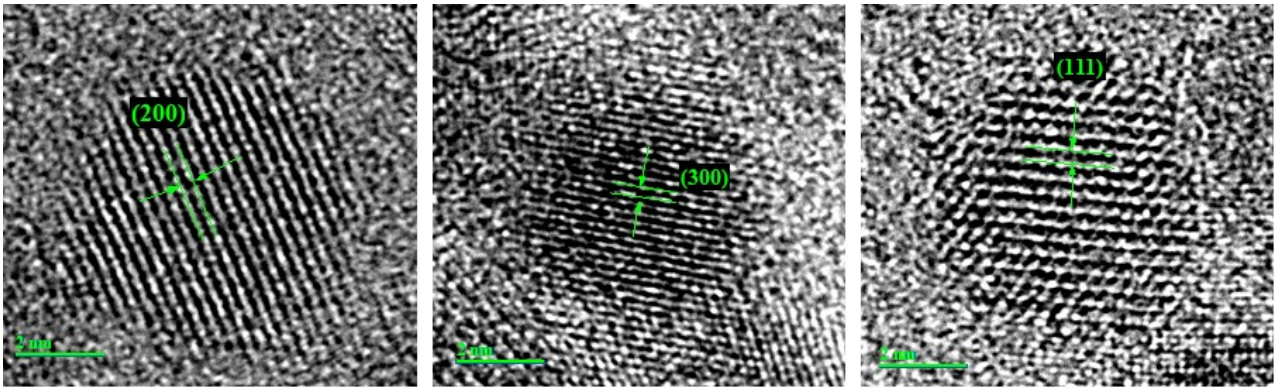

Figure S6: Atomic resolution for NCs in PbS-EDT.

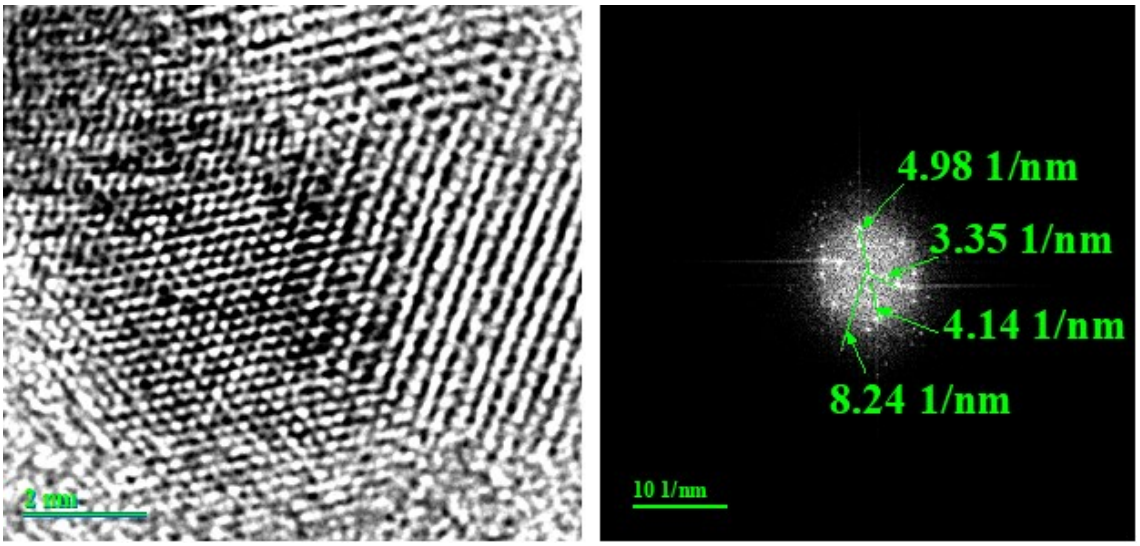

Figure S7: Atomic resolution for NCs in PbS-EDT.

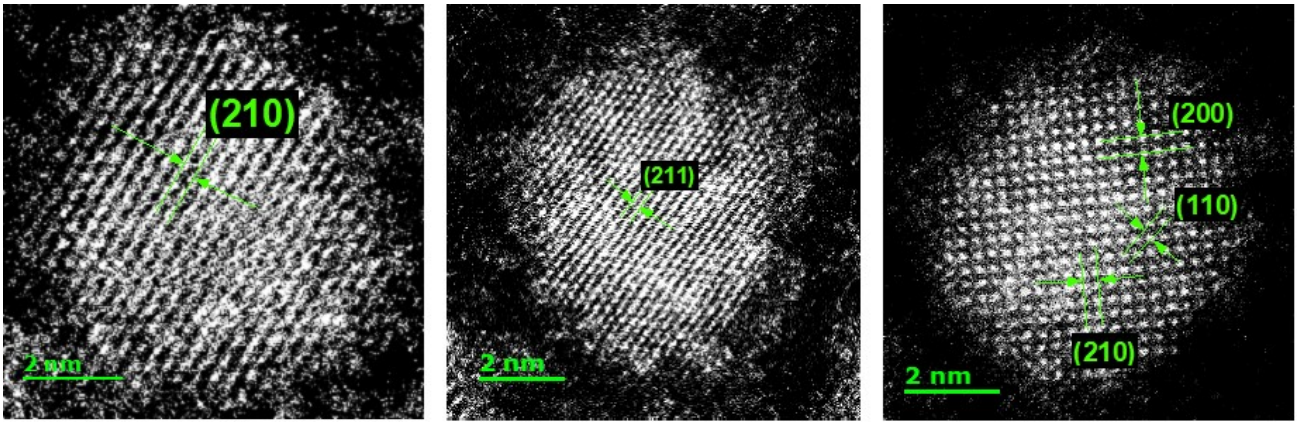

Figure S8: Atomic resolution for NCs in PbS-TBAI.

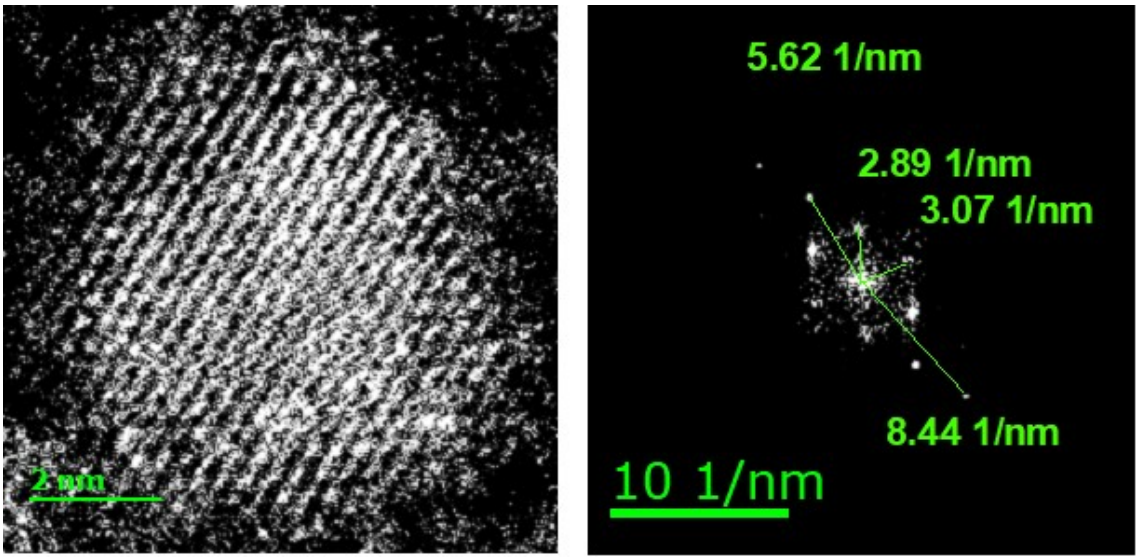

Figure S9: Atomic resolution for NCs in PbS-TBAI.

Table S2: List of planes from the FFT of atomic resolution images of PbS-EDT and PbS-TBAI.

FFT (1/nm)	Lattice planes
PbS-EDT	
3.35	(200)
3.46	(111)
4.14	(211)
4.98	(300)
8.24	(422)
PbS-TBAI	
2.89	(111)
3.07	(200)
5.62	(311)
8.44	(510),(431)

4 Effective Dielectric Constant

The filling factor or the volume fraction θ has been estimated from the TEM images for closed packed spheres. As the NCs are distributed randomly, it was therefore necessary to calculate the interparticle distances among NCs and their radii. The permittivity in Figure S10 for COINs were dedicated accordingly from the Maxwell-Garnett effective medium theory which is mentioned in the main manuscript. The permittivity of COINs, excitonic energy and the transport energy of different ligands are listed in Table S3. The optical energy gap for PbS is found to be equal to 0.78 eV from the absorption spectrum of NCs, Figure S1b.

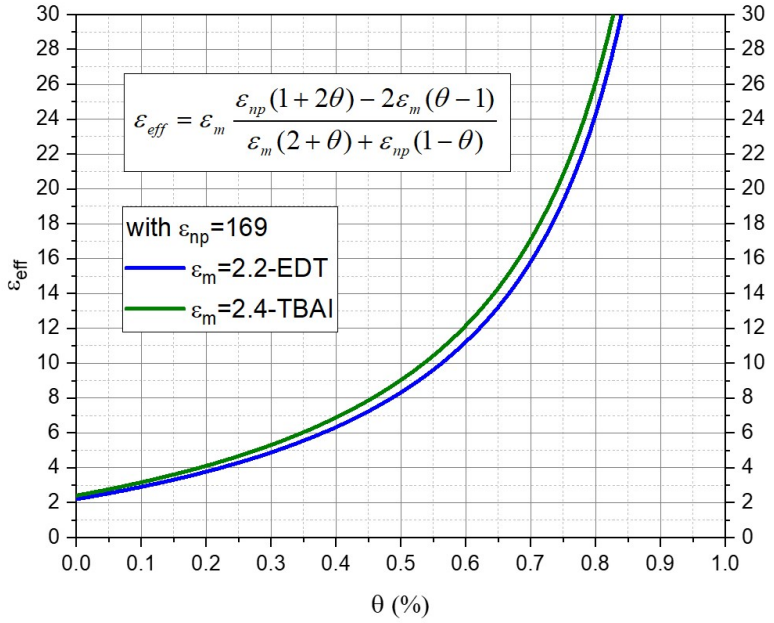

Figure S10: Calculated effective dielectric constant for COINs with different ligands.

Table S3: The dielectric constants for COINs.

COINs	ε_{m}	$\varepsilon_{\mathrm{np}}$	$\varepsilon_{\mathrm{eff}}$	$Eg_{\mathrm{transport}}$ (eV)	E_{exciton} (meV)	θ
PbS-EDT in acetontrile	2.2	169	18.5	0.82	44.5	0.74
PbS-TBAI in methanol	2.4	169	17	0.82	48.4	0.7

The effective dielectric constants of COINs with variant ligands were calculated according to the Maxwell-Garnett effective medium theory (1):[?]

$$\epsilon_{eff} = \epsilon_m \frac{\epsilon_{np}(1+2\theta) - 2\epsilon_m(\theta-1)}{\epsilon_m(2+\theta) + \epsilon_{np}(1-\theta)}, \tag{1}$$

ε_{m} represents the optical permittivity of the ligand, θ is the fraction of the volume filled with nanoparticle, $\varepsilon_{\mathrm{np}}$ is the nanoparticles permittivity.

5 Ligand Concentrations

To test the ideal ligand concentrations for device performance, different concentrations were used to prepare the photodiodes. In the case of the EDT ligand, the highest values of open circuit voltage and short circuit current were observed at a concentration of 30 mM. However, different findings for TBAI ligand were obtained. There was no remarkable trend change at the photodiode parameters by increasing the concentration. Therefore, we used a concentration of (10mg/ml) which is equal to (27mM) as mentioned in the published reference.[?] It is important here to mention that the concentration of the PbS-NCs is (1.25mg/ml) in this experiment.

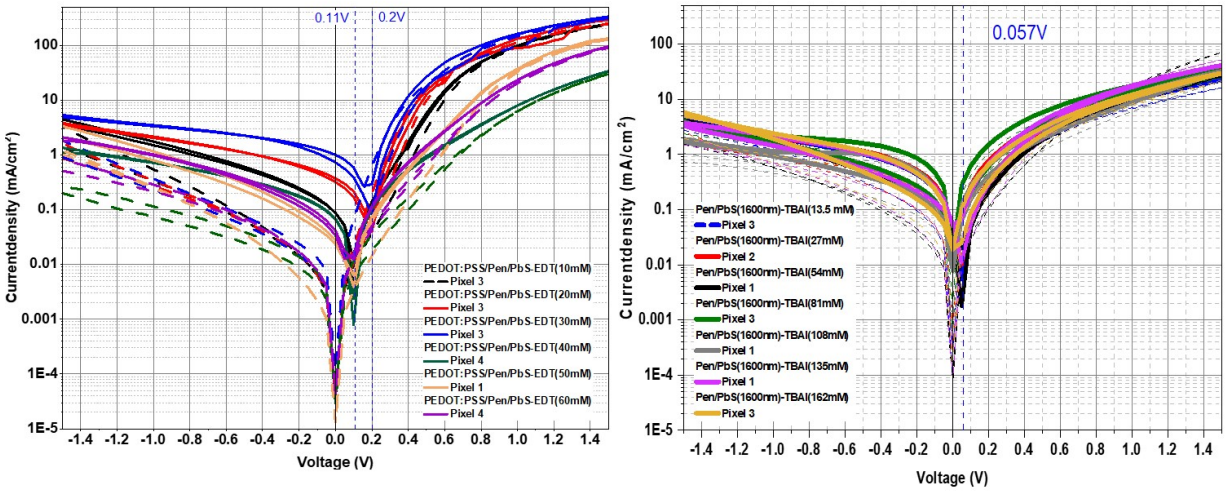

Figure S11: a) J-V characteristics for different a) EDT concentrations, b) TBAI concentrations.

6 Reproducing Pixels

It was possible to reproduce samples of the normal stacks with very similar results for all of the pixels (Figure S12). This achievement suggests homogeneous films, homogeneous photo generation and collecting of charge carriers. Here, the concentration of the PbS-NCs

is (1.25mg/ml) for all samples and the concentration of the EDT is 30mM.

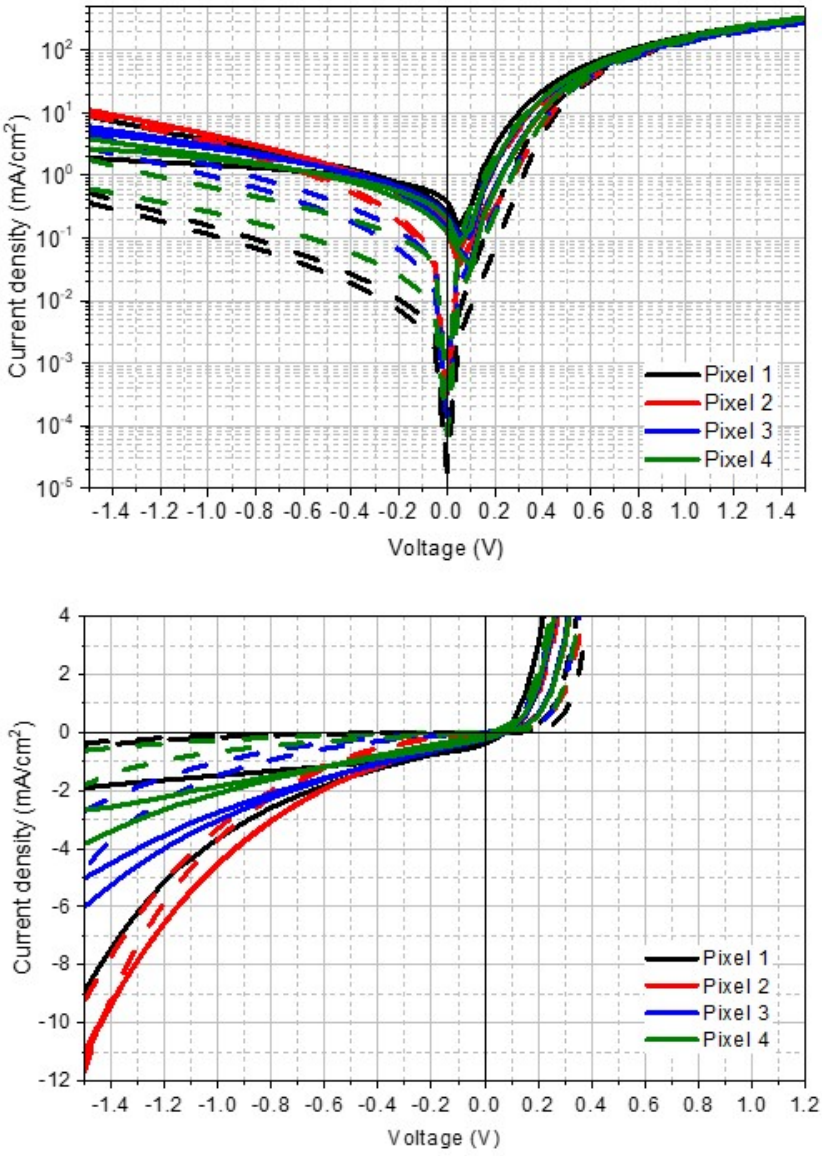

Figure S12: Normal stacks with PEDOT:PSS/pentacene/PbS-EDT(10mM)/BCP/Al